

A TWO-STAGE CIRCUMFERENTIAL SLOT VIRTUAL IMPACTOR FOR
BIOAEROSOL CONCENTRATION

A Thesis

by

REFUGIO REY ISAGUIRRE IV

Submitted to the Office of Graduate Studies of
Texas A&M University
in partial fulfillment of the requirements for the degree of
MASTER OF SCIENCE

May 2005

Major Subject: Mechanical Engineering

A TWO-STAGE CIRCUMFERENTIAL SLOT VIRTUAL IMPACTOR FOR
BIOAEROSOL CONCENTRATION

A Thesis

by

REFUGIO REY ISAGUIRRE IV

Submitted to Texas A&M University
in partial fulfillment of the requirements
for the degree of

MASTER OF SCIENCE

Approved as to style and content by:

Andrew R. McFarland
(Chair of Committee)

Dennis L. O'Neal
(Member)

Yassin A. Hassan
(Member)

Dennis L. O'Neal
(Head of Department)

John S. Haglund
(Member)

May 2005

Major Subject: Mechanical Engineering

ABSTRACT

A Two-Stage Circumferential Slot Virtual Impactor for

Bioaerosol Concentration. (May 2005)

Refugio Rey Isaguirre IV, B.S., Texas A&M University

Chair of Advisory Committee: Dr. Andrew McFarland

Slot virtual impactors provide an efficient low power method of concentrating aerosols. A circumferential slot virtual impactor (CSVI) is especially effective because it has a continuous slot, and, therefore, has no losses associated with the ends of the slot. A CSVI can also fit a longer slot in a smaller footprint than a linear slot virtual impactor.

A two-stage circumferential slot virtual impactor system has been designed and tested. The CSVI units are similar in principle to that tested by Haglund and McFarland (2004). Specific geometric changes to the nozzle region were introduced based on the numerical models of Hari (2005). The greatest change to the nozzle geometry of Haglund and McFarland (2004) is the introduction of a radius on the accelerator nozzle. The radius on the accelerator section allows larger particles to make a smoother transition into the focused jet. The smoother transition reduces the amount of wall losses for larger particles.

The geometric changes show a significant increase in the particle size range that the virtual impactor can effectively concentrate. The extension of the dynamic range of the improved geometry was evident in the results for both the 100 L/min first stage and the 10 L/min second stage CSVI units. The two stages were tested individually and in series where the nozzle Reynolds number was 250 for both units.

The results of the experiments on the two stage CSVI system showed a peak collection efficiency of 90%. The first and second stage had a Stokes cutpoint of 1.2, corresponding to a particle size of about 2.5 μm .

ACKNOWLEDGEMENTS

Funding for this study was provided by the U.S. Army Research, Development, and Engineering Command (RDECOM), Edgewood Chemical Biological Center (ECBC), under supervision of Dr. Edward Steubing and Dr. Jerry Bottiger (Texas Engineering Experiment Station, Contract Number 32579-60240.)

I would also like to extend a heartfelt thank you to my advisor, Dr. Andrew McFarland, for his guidance throughout my studies. I am also grateful to my committee members and all of my colleagues at the Aerosol Technology Laboratory especially those who worked with me directly on this project: Dr. John Haglund, Dr. Sridhar Hari, Shawn Conerly, Clint Adams, Satya Seshadri, John Vaughan, and Michael Wiley.

TABLE OF CONTENTS

	Page
ABSTRACT.....	iii
ACKNOWLEDGEMENTS.....	v
TABLE OF CONTENTS.....	vi
LIST OF TABLES.....	viii
LIST OF FIGURES.....	ix
INTRODUCTION.....	1
THEORY.....	4
LITERATURE REVIEW.....	8
DESIGN.....	13
Prototype.....	13
Acoustic Disturbance.....	14
TOLERANCE VERIFICATION.....	16
EXPERIMENTAL PROCEDURE.....	17
DISCUSSION OF ERRORS.....	20
RESULTS.....	26
Pressure Drop vs Flow Rate.....	26
Efficiency Curves.....	27
First Stage.....	27
Second Stage.....	28
1 st and 2 nd Stage CSVI in Series.....	28
Effect of Exposure to the Ambient Air of the CSVI Units.....	28
SUMMARY AND CONCLUSIONS.....	30
FUTURE RECOMMENDATIONS.....	31
REFERENCES.....	32
APPENDIX.....	36

VITA.....54

LIST OF TABLES

	Page
Table 1: Uncertainties used for Kline McClintock Uncertainty Analysis.....	52
Table 2: Measurements from first stage CSVI.....	53

LIST OF FIGURES

	Page
Figure 1: Principle of virtual impaction.....	3
Figure 2: Photograph of CSVI stage 1 and 2.....	37
Figure 3: Inside of first and second stage CSVI units.	38
Figure 4: Acoustic absorbing open face foam in the center of the first stage CSVI.....	39
Figure 5: Rubber casting of the first stage critical region.....	40
Figure 6: Measured values compared to designed values for stage 1 CSVI.....	41
Figure 7: CSVI aerosol sampling chamber.....	42
Figure 8: Complete flow system for CSVI stage 1 and 2.....	43
Figure 9: Predicted uncertainty in Stokes calculation by Kline-McClintock.....	44
Figure 10: Pressure drop vs flow rate for first stage CSVI.....	45
Figure 11: Illustration of crossing trajectories of larger particles.....	46
Figure 12: Performance of the first stage CSVI.....	47
Figure 13: Performance of second stage CSVI.....	48
Figure 14: Comparison of first and second stage CSVI units.....	49
Figure 15: First and second stage CSVI plots.....	50
Figure 16: Demonstration of ability of second stage to be nested within the first stage..	51

INTRODUCTION

Biological terrorism is a major threat to the national security of the United States of America. Real-time detection of aerosolized biological agents is necessary in order to minimize the size of the population exposed and to initiate available countermeasures. An example of a countermeasure is the administration of the oral antibiotic ciprofloxacin which is known to be an effective treatment for exposure to Anthrax (*Bacillus anthracis*).

To detect a low concentration of a biological agent in the environment with contemporary near-real-time sensors, a relatively large volume of air must be sampled in comparison with the normal rate of respiration for humans. The need for sampling a high volume of air arises from the low amounts of agent that can do a human harm and the relatively low resolution of detection capabilities. The particles contained in the large volume of air must be concentrated into a smaller fluid volume before it can be checked for harmful agents. The particles are usually concentrated and collected in a low flowrate liquid medium because current detection capabilities require a hydrosol. A virtual impactor concentrates the particles in a flow into a smaller stream. The virtual impactors that were the focus of this study were designed for use with the Aerosol to Hydrosol Transfer Stage (Phan and McFarland 2004). In the future it may be possible to detect biological agents without first suspending them in a liquid; an application for which a virtual impactor would be a natural fit.

One device that has been employed for the concentration of biological particles is a cyclone. The cyclone has been shown to be an effective concentrator, but to collect the

This thesis follows the style and format of *Aerosol Science and Technology*.

small-sized particles that are anticipated to be associated with bioagents (e.g. 1 to 10 μm aerodynamic diameter, AD), a cyclone requires a relatively large amount of power to operate (Moncla 2004) in comparison to concentration of particles with a properly designed virtual impactor. The first stage virtual impactor of this study with a particle size cutpoint of 2.5 operates with 20 times less power consumed per liter sampled than a cyclone with a cutpoint of 1.5 μm . With a slot virtual impactor, there exists the potential to reduce the cutpoint without significantly increasing the power consumption of a detection system. The replacement of cyclones with virtual impactors as an aerosol concentrator would considerably reduce the power consumption of a biological detection unit.

A virtual impactor concentrates aerosol particles by accelerating a flow through a nozzle producing a jet. Ninety percent of the flow is then forced by the nozzle geometry and flow control to undergo an abrupt change in direction while the remaining ten percent of the flow, the minor flow, continues on a straight path into an opposed collection nozzle. Relatively larger particles have sufficient inertia to penetrate the curvature of the gas streamlines and continue on the straight path into the collection nozzle. The concept of virtual impaction can be seen in Figure 1. In the absence of particle wall losses, the minor flow will contain the same number of the particles present in the flow entering the virtual impactor and will have a number concentration ten times the entrance concentration. A virtual impactor operating with this ratio of minor-to-entrance flow and without nozzle wall losses is said to have a concentration factor of 10. A two stage virtual impactor operating under the same conditions would have 100 times the

concentration of the initial inlet flow. In some cases it may be necessary to add a third stage of concentration in order to increase the signal to a bioaerosol detector.

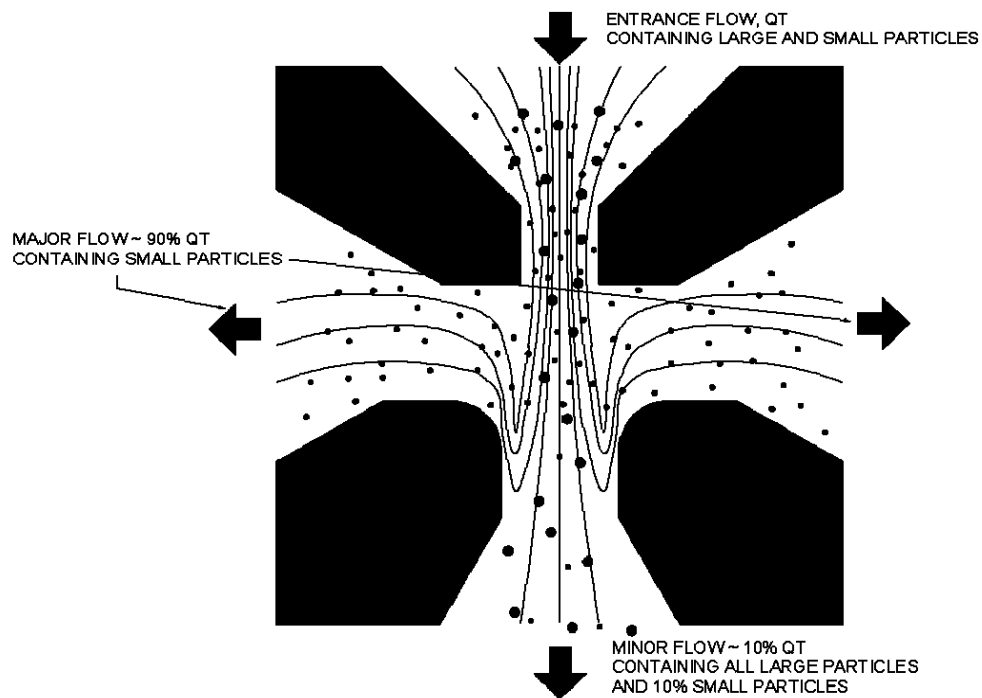


Figure 1: Principle of virtual impaction

THEORY

The behavior of a virtual impactor can be characterized based on two non-dimensional parameters, the Stokes and Reynolds numbers.

$$Stk_{L_c} = \frac{\rho_p \cdot D_p^2 \cdot C_c \cdot U_o}{18 \cdot \mu_f \cdot L_c} \quad [1]$$

$$Re_{L_c} = \frac{\rho_f \cdot U_o \cdot L_c}{\mu_f} \quad [2]$$

where ρ_p is the particle density, ρ_f is the fluid density, D_p is the particle diameter, C_c is the slip correction factor, U_o is the mean velocity at the exit of the accelerator section, μ_f is the dynamic viscosity of the fluid, and L_c is either the jet width or half the jet width.

For a rectangular jet virtual impactor the Stokes number is defined in common practice as the ratio of the particle stopping distance at the mean nozzle exit velocity to half the jet width while for the Reynolds number the full jet width is used. The Stokes number is the single most important parameter that governs the behavior of particle motion in a virtual impactor.

The Reynolds number may also play an important role in the performance of the virtual impactor. Marple and Chien (1980) has shown dependence on the cutpoint for real surface impactors with Reynolds number owing to the slight difference in velocity distribution across the impaction nozzle for $Re < 1000$. Furthermore, there are

potentially instabilities that may occur in the virtual impactor that may vary significantly with Reynolds number. Apart from these phenomenons, the performance of a virtual impactor is nearly independent of the Reynolds number as will be observed below.

The ideal power required to operate a virtual impactor is dependant only on the pressure drops across the major and minor flows of the concentrator. The ideal power consumption for the virtual impactor is calculated by taking the product of the pressure drop and the flow rate.

$$\dot{W}_{Ideal} = Q \cdot \Delta P \quad [3]$$

where \dot{W}_{Ideal} is the ideal power consumption of the virtual impactor. ΔP is the pressure drop across the virtual impactor in the major and minor flows, and Q is the volumetric flow rate. The largest component of the power consumption is the major flow pressure drop because that accounts for 90% of the total flow rate. The major flow pressure drop is proportional to the square of the product of the mean velocity at the accelerator nozzle and the density of the fluid squared. The proportionality constant, K , is referred to as the pressure coefficient.

$$\Delta P = K \frac{\rho_f \cdot U_o^2}{2} \quad [4]$$

The mean throat velocity is the ratio of the volumetric flow rate to the total slot area.

$$U_o = \frac{Q}{2 \cdot L_c \cdot \pi \cdot d} \quad [5]$$

where the product $2 \cdot L_c \cdot \pi \cdot d$ gives the total slot length of a circumferential slot of diameter d . It should be noted that the diameter and total flow rate are coupled for a CSVI with fixed cutpoint and nozzle geometry.

To minimize the power consumption of a virtual impactor at a fixed flow rate, it is necessary to minimize the pressure drop. Substituting U_o from Equation [5] into Equation [4] yields Equation [6]:

$$\Delta P = \frac{K \cdot \rho_f \cdot \left(\frac{Q}{2 \cdot L_c \cdot \pi \cdot d} \right)^2}{2} \quad [6]$$

Substituting Equation [5] into Equation [1] yields Equation [7]:

$$Stk_{L_c} = \frac{\rho_p \cdot D_p^2 \cdot C_c \cdot \left(\frac{Q}{2 \cdot L_c \cdot \pi \cdot d} \right)}{18 \cdot \mu_f \cdot L_c} \quad [7]$$

From Equation [6] it can be seen that for a fixed flow rate, only two user definable parameters can be varied to minimize the pressure drop, L_c and d . Of L_c and

$$Stk_{L_c} = \frac{\rho_p \cdot D_p^2 \cdot C_c \cdot \left(\frac{Q}{2 \cdot L_c \cdot \pi \cdot d} \right)}{18 \cdot \mu_f \cdot L_c}$$

d ,

[7] shows only parameter that reduces the pressure drop without decreasing the Stokes number is the slot width L_c .

The extent to which L_c can be minimized is dependent on the ability to manufacture the virtual impactor. As the slot width is reduced, the virtual impactor becomes increasingly sensitive to misalignment of the accelerator and receiver nozzles. Before selecting a slot width, one must consider the capabilities of contemporary manufacturing to hold the required tolerances. Previous studies with round jet nozzles

(Loo and Cork, 1988) suggest that the maximum allowable misalignment between the accelerator and the receiver nozzles is 5% of the accelerator dimension. For the present study, a slot width of 0.000508 meters (0.020") was selected. In order to satisfy the 5% maximum misalignment, the components that form the virtual impactors must interface to result in an alignment within 0.0000254 meters (0.001").

LITERATURE REVIEW

The concept of virtual impaction has origins in the more traditional approach of separation of particles according to size by inertial impaction on a real surface. Inertial impaction is an effective way to separate larger more massive particles from a flow. Inertial impaction originated in the years 1860-1877 and was effectively used to impact particles on a slide for observation under a microscope. The inertial impactor led to several other aerosol instruments capable of separating larger particles from smaller ones (Marple 2004).

Hounam and Sherwood (1965) eliminated the problems associated with particle bounce and saturation in an inertial impactor by eliminating the impaction surface. Instead of a solid impaction surface, particles that have sufficient inertia to separate from the incident stream lines continue into an orifice that slowly draws the “impacted” particles to a collector or analyzer.

Several theoretical studies have been completed regarding the behavior of virtual impactors. Ravenhall et al. (1978, 1982) studied virtual impactors by applying classical fluid dynamics to the internal flows. Several geometrical parameters were demonstrated to significantly change the behavior of the virtual impactor when varied. Their studies also began to demonstrate the sensitivity of a virtual impactor to relatively small geometrical changes. Further evidence of the sensitivity of virtual impactors to relatively minor geometric changes was presented by Marple and Chien (1980). A mathematical model of a counterflow virtual impactor was created by Lin and Heintzenberg (1995). Forney et. al (1982) studied the effects of various geometric and physical parameters on

the efficiency of a virtual impactor. Asgharian and Godo (1997) used a finite element analysis to model the behavior of spherical particles and fibers in a virtual impactor designed by Chien and Lundgren (1993). The numerical models showed good agreement with the experimental results. Han and Moss (1997) used dye to trace the streamlines in a virtual impactor.

Round jet virtual impactors have been the subject of extensive research. Round jet virtual impactors are easily manufactured and provide an effective method for the concentration of aerosol particles. One application of the round jet virtual impactor is that of Chang et. al (2002) who used a high volume round jet virtual impactor to concentrate particles in the ambient air. A separate application of a round jet virtual impactor was developed by Sioutias et. al (1999) in which a round jet virtual impactor was used to concentrate ultra fine particles by first inducing growth of the ultra fine particles by condensation of water vapor in a supersaturated environment. The water droplet that forms around the particle significantly increased its mass and ability to be concentrated. The minor-to-total flow ratio was studied, and it was found that decreasing the minor flow from 20% to 10% caused no significant change in the collection efficiency.

An improved round jet virtual impactor was studied by Masuda et. al (1979). The improvement was made by using a clean air core to prevent the losses associated with the aerosol being in contact with the impactor wall and to eliminate small particles from the minor flow stream. Chen and Yeh (1987) used a clean air core virtual impactor and experimentally achieved less than 5% wall losses. A clean air core round jet virtual

impactor was applied to determine the size of the particles in an aerosol generator by Chein and Lundgren (1993,1995).

Among the most significant work regarding round jet virtual impactors was published by Loo and Cork (1988) who studied the sensitivity of round jet virtual impactor to different geometrical parameters. Their experiments provide a feeling of what parameters are the most critical for a virtual impactor. One critical parameter noted in their studies was the relative alignment between the accelerator nozzle and the receiver collection probe.

Romay et. al (2002) designed and experimentally examined a multiple jet round nozzle virtual impactor for use in the concentration of bioaerosols. They were able to develop a multiple stage virtual impactor and achieved a concentration of 150-270 times the ambient concentration. In this case, the virtual impactor had a cut point of about $2\mu\text{m}$. A limitation to the applicability of their concentrator is the range of particle sizes it can collect at a fixed flow rate. At approximately 300 L/min, the concentrator was above 80% efficient for particles ranging from about 3- $6\mu\text{m}$ AD.

Slot virtual impactors are preferred for high volume aerosol concentration. A single slot can replace an array of round jet virtual impactors. A single effective design of a slot nozzle virtual impactor can accommodate arbitrary flow rate while maintaining constant cut point by varying the slot length. Ding and Koutrakis (2000) developed and conducted experiments with a slit nozzle virtual impactor. They studied the effect that the Reynolds number has on the collection efficiency of the virtual impactor and recommended an accelerator to receiver ratio between 1.2 and 1.7.

Sioutas et. al (1994a) developed a slit virtual impactor with a cutpoint below $0.25\mu\text{m}$. The virtual impactor had relatively few particle losses for a size range from $0.05\text{-}2\mu\text{m}$ particles. For their virtual impactor the pressure drop at a sampling rate of 15 L/min was 8.7 KPa (35" H₂O) and 18.4 KPa (74" H₂O) at 24 L/min. Another application of this virtual impactor was the separation of atmospheric particulate from gaseous pollutants, Sioutas et. al (1994b). Haglund et. al (2002) evaluated a high volume aerosol concentrator. Their results showed a peak collection efficiency in the minor flow of about 80% and a useable particle size range from about $3\text{-}10\mu\text{m}$. Ding et. al (2000) developed a high volume slot virtual impactor with a similar useable range.

Haglund (2003) and Haglund and McFarland (2004) designed, constructed and characterized a new geometrical arrangement for a slot nozzle virtual impactor: a circumferential slot virtual impactor (CSVI). In this study various nozzle configurations were tested and developed, supported by numerical modeling and optimization of the virtual impactor nozzle geometry (Hari, 2003). The numerical models were used to study the effect of misalignment on a virtual impactor as well as to optimize certain nozzle parameters. Good agreement was observed between the numerical simulations and results. The experimental device showed a minimum of 72% collection efficiency for particles ranging from twice the cutpoint size (approximately 3.5 mm AD) to $10\mu\text{m}$ AD. Also noted in this study was that under some operational conditions of a virtual impactor, an acoustic instability could arise leading to a drastic decrease in the collection efficiency.

Based on the numerical and experimental work on the CSVI described immediately above, a new virtual impactor nozzle geometry was developed. This

optimized geometry was incorporated into prototype units fabricated by TSI (Minneapolis, MN) and has been integrated into the CSVI units that are the subject of the present study.

The focus of this study was a two stage circumferential slot virtual impactor for use in bioaerosol concentration. For the present study, the minor-to-total flow ratio was fixed at 10% for each stage. The two-stage circumferential slot virtual impactor studied was shown to be both relatively low-power and highly efficient in comparison to cyclones as well as other virtual impactors..

Previous studies have shown that the particle size distribution for which a virtual impactor is effective can be limited by the geometry of the virtual impactor. Previous virtual impactors have experienced an efficiency drop as the particles become larger than $5\mu\text{m}$ which reduces the working size range (Haglund 2003). A major focus of this study was incorporating a new optimized geometry to expand the usable performance envelope of the virtual impactor over a greater particle size range at a fixed flow rate.

DESIGN

Prototype

The numerical models run by Hari (2005) were incorporated into the updated virtual impactor. The primary motivation for the geometric changes was the losses experienced at higher Stokes numbers. The losses of particles twice the cutpoint can be attributed to crossing trajectories that occur as the aerosol is accelerated through the nozzle.

In addition to the geometric changes to the critical zone, the virtual impactors were designed to operate at 100 L/min for the first stage and 10 L/min for the second stage. The result of the two stages is a concentrator that samples 100 L/min and reduces the flow to 1 L/min achieving up to 100 times the initial concentration. The first and second stage units were designed to have an identical mean velocity at the accelerator nozzle and with identical critical geometries. The result is two virtual impactors which have the same Stokes 50 cutpoint as well as the same aerodynamic particle size cutpoint. The major difference between the first and second stage CSVI is that the second stage nozzle lies on one tenth the diameter that it does in the first stage. Photographs of the first and second stage CSVI units can be found in Figure 2 and Figure 3.

In order to characterize the CSVIs with monodisperse aerosols each unit rested in an aerosol sampling chamber (Figure 7). The chamber has four interfaces with other components. First, the chamber has an inlet to allow the aerosol in. The chamber also has two holes on its side through which the two major flows are removed from the

impactor. The final interface is a single port located on the underside of the sampling chamber through which the particle rich minor flow can be removed from the system. The same principle was applied to the second stage CSVI which has one tenth the flow rate. The 10 L/min minor flow from the first stage CSVI behaves as the inlet for the second stage.

There was initial concern regarding this method of experimentation because as the air is sampled through the radial-feed CSVI units, it is forced to make a turn before it enters the virtual impactor. The turn raised the possibility that some of the larger particles were lost before they entered the CSVI. To investigate this possibility a reference was conducted with a “blank inlet.” The blank inlet was constructed with the same physical characteristics as the CSVI units minus the accelerator and receiver blades. The blank was intended to force 100 L/min to make a turn as if it was going to enter the CSVI without the flow undergoing any concentration. The air was then collected on a glass fiber filter and compared to 100 L/min collected with the usual inline glass fiber filter. The results showed no statistical difference between the “blank inlet” reference and the standard inline filter reference for particles up to 12 μm . These results verified that no significant losses can be attributed to the turn the flow takes to enter the CSVI units.

Acoustic Disturbance

The generation of an audible acoustic wave may be detrimental to the efficiency of a virtual impactor (Haglund and McFarland 2004). An audible high-pitched acoustic wave is generated in the first stage CSVI when it is operated at its standard flow rate of 100 L/min. To dampen the sound a small piece of adhesive-backed open face foam was

placed opposite the minor flow. Figure 4 shows the placement of the acoustic absorbing open-faced foam. It was observed that the insertion of foam eliminated the audible sound emanating from the first stage CSVI. The second stage does not generate an audible acoustic wave at its standard operating condition of 10 L/min.

TOLERANCE VERIFICATION

The behavior of a virtual impactor is heavily dependant on the accelerator to receiver alignment (Haglund 2003). It is critically important to verify the tolerances of a virtual impactor. The resolution required to make these measurements make traditional tolerance verification methods insufficient. Direct optical measurement with a microscope is impossible because in an assembled CSVI only the receiver nozzle is visible.

Rubber compound (Flexbar reprotubber Islandia, NY) was used to make a cast of the critical zone. The cast was then sliced and measured under a microscope by comparing the results to a known standard. The method was validated on a surface that was directly measurable using an optical microscope. A map of eight points around the nozzle of the first stage was taken and an average value of accelerator to receiver nozzle misalignment was determined to be 2%. The second stage was mapped in only two places which resulted in an average of 2% misalignment. A photograph of a typical critical zone mold is shown in Figure 5. The results of the thorough survey can be found in appendix Table 2. Figure 6 shows the measured values of the first stage virtual impactor compared to the designed values.

EXPERIMENTAL PROCEDURE

The experimental procedure for determining the collection efficiency of the virtual impactors can be divided into two steps.

- 1.) Monodisperse aerosol generation and experimental protocol.
- 2.) Analysis of samples

Particles smaller than 3 μm AD can be generated by atomizing a hydrosol containing polystyrene spheres that are tagged with a fluorescent tracer (Duke Scientific, Palo Alto, California). The microspheres are first suspended in water with a surfactant and then aerosolized with a Collison atomizer (CN31i, 6jet, BGI incorporated, Waltham, Massachusetts).

Larger oleic acid liquid particles can be generated using a vibrating orifice aerosol generator, VOAG (Model 345001, TSI Inc., St. Paul, Minnesota). The oleic acid is dissolved in ethanol and tagged with a fluorescent tracer, sodium fluorescein. The physical size of the aerosol particles is determined by impacting them on a glass slide that is coated with an oil-phobic agent (3M Co. Chemical FC-721) and optically measuring the particles with a microscope. The size observed under the microscope is corrected for flattening using a correction factor developed by Olan-Figueroa et. al. (1982). The aerosol is monitored for quality assurance purposes with an Aerodynamic Particle Sizer (APS Model 332100, TSI., St. Paul, Minnesota).

The efficiency of a unit is determined by generating a monodispersed aerosol and drawing it into the CSVI test fixture, which consists of an 8 inch PVC tube that has been capped on one end and modified to allow the major and minor flow streams to exit the tube, Figure 7. The particle rich minor flow stream (10% of total flow) is filtered via an

in line glass fiber filter (47mm A/D Glass Fiber filter Ann Arbor, Michigan). At the completion of the test, the minor flow filter of the CSVI is placed in a jar and set aside. The concentrator is then removed and a fresh inline glass fiber filter is used to filter the entire flow rate without the aerosol concentrator. If the CSVI is 100% efficient, the 10% minor flow filter and the 100% reference filter will have the same amount of particles on them.

The collection filters are then soaked in a solvent to release the fluorescent dye from the particles. Filters containing liquid oleic acid particles were soaked in a 50/50 blend of distilled water and isopropyl alcohol for a minimum of 8 hours. Trace amounts of sodium hydroxide was added to the solution to stabilize the variation in the fluorescence from a variation in the PH. The glass fiber filters with solid polystyrene latex spheres were soaked in ethyl acetate for a minimum of 30 minutes. The solution is then analyzed with a fluorometer (Turner Quantech Digital Filter Fluorometer Model FM109515, Barnstead International, Dubuque, Iowa). The fluorescence from the minor flow filter solution can be compared to the fluorescence of the reference filter solution to determine the collection efficiency.

The flow system used to characterize the two stage CSVI units can be seen in Figure 8. Each flow in the virtual impactor is measured independently by a rotameter and the total flow is measured by the total flow rotameter. The flow system as drawn was used to characterize the first and second stage CSVI units independently. Then the two stage virtual impactor was characterized as a system. The reference samples for each unit were conducted by closing the valves on the major and minor flows and opening the appropriate reference valve. This method of taking reference filters allow the virtual

impactor and the reference to be taken with minimal change to the overall flow system. The reference flow rate and the total flow rate for the CSVI experiments were measured by the same rotameter.

Every reasonable measure to ensure the quality and reliability of the experiments were taken. The discussion of errors section provides a more detailed account of the steps taken to minimize the error. An estimate of the uncertainty is also made.

DISCUSSION OF ERRORS

The errors associated with the results obtained in this study can be separated into two sections: Systematic errors and precision errors. The systematic errors refer to inherent experimental issues associated with the way the experiment was conducted or from the experimental set up. It should be noted that all reasonable steps have been taken to minimize systematic errors.

One potential systematic error is the presence of a leak in the flow system used to control the CSVI units. A leak in the flow system could cause drastic inaccuracies in the collection efficiency's associated with the virtual impactors. To minimize the possibility of this potential error the entire flow system was constructed with National Pipe Taper Threads, Swagelok brand compression fittings (swagelok.com), and Flexible Polyethylene Tubing (mcmaster.com). All components when used properly will hold a vacuum of a minimum of 1.5 bar gauge.

To ensure that all components were properly used a leak check of the entire system was performed. To perform the leak check, the plumbing system was disconnected from the virtual impactor and all free ends were plugged with a rubber stopper. The system was determined to be leak free if it could maintain a vacuum of 40 inches of water for 30 seconds.

Another type of systematic error could occur if the dishes used to soak the glass fiber filters in a solvent were not sufficiently clean. The presence of residual fluorescence from previous tests could also have detrimental effects on the experimental

results. As a result, two different dish cleansing procedures were established for the two types of particles made and solvents used.

In the case of the solid polystyrene latex spheres, the solvent used to dissolve the spheres is ethyl acetate. Ethyl acetate is not soluble in water in large quantities, but is soluble in isopropyl alcohol. In order to ensure that the containers are clean following the experiments, after the bulk of the ethyl acetate is removed from the container, it is rinsed with isopropyl alcohol. The remaining liquid in the container is a mixture of trace ethyl acetate and isopropyl alcohol that is soluble in water. The container is then rinsed a minimum of ten times with tap water and allowed to air dry. The filters with impacted oleic acid particles are soaked in a mixture of isopropyl alcohol and distilled water with trace amounts of sodium hydroxide. Once the bulk of the solution is removed from the container, the container is then rinsed a minimum of ten times with tap water and is allowed to air dry.

To assure that the experiments are not influenced by preexisting fluorescence in the containers, a few trial containers that had been cleaned using the procedure described above were filled with a sample solution and its fluorescence was measured at a typical gain. Background noise from preexisting fluorescence on the containers was not any higher than the background for isopropyl alcohol and water or ethyl acetate placed in a new cuvette.

The same experimental setup and procedure was used for both the virtual impactors and the reference samples taken. It can be assumed that as a result any other systematic errors would be present in both the reference and virtual impactor samples, minimizing their significance.

The second major type of error can be quantified as a precision error. These errors are the result of our resolution to measure certain parameters that are important in the determination of the experimental results. Examples of precision errors are our ability to measure the volumetric flow rate, the volume of solvent the glass fiber filters are soaked in, and the precision of the fluorometer. These errors will propagate and cause an overall level of uncertainty for specific data points. The uncertainty will be evaluated based on the Kline & McClintock method. There are two calculations that affect the experimental data. First is the error associated with the Stokes number, and second is the uncertainty associated with the efficiency calculations.

The Kline McClintock uncertainty analysis method is defined as:

$$\delta R = \left[\sum_{i=1}^M \left(\frac{\partial R}{\partial \hat{X}_i} \delta \hat{X}_i \right)^2 \right]^{\frac{1}{2}} \quad [8]$$

where

δR = Uncertainty associated with the calculation R.

\hat{X}_i = Variable

$\delta \hat{X}_i$ = Uncertainty associated with the variable \hat{X}_i

The first uncertainty calculation is the dimensionless Stokes number.

Substituting

$$U_o = \frac{Q}{2 \cdot L_c \cdot \pi \cdot d}$$

and

$$C_c = 1 + 2.52 \frac{\lambda}{D_p} \quad [9]$$

into Equation [1] yields

$$Stk_{L_c} = \frac{\rho_p \cdot D_p^2 \cdot Q \cdot \left(1 + 2.52 \frac{\lambda}{D_p}\right)}{36 \cdot \pi \cdot d \cdot \mu_f \cdot L_c^2} \quad [10]$$

The parameters that were measured during the experiment are L_c, D_p, Q . All other parameters resulted from tabulated values in a text, e.g. viscosity of air at STP and the mean free path of air, it is assumed that errors associated with these values are negligible. The calculation of the uncertainty in the Stokes number calculation follows:

$$\frac{\partial Stk_{L_c}}{\partial Q} = \frac{Stk_{L_c}}{Q} \quad [11]$$

$$\frac{\partial Stk_{Lc}}{\partial D_p} = \frac{Stk_{Lc}}{D_p} \left[\frac{2.52 \lambda + 2 D_p}{2.52 \lambda + D_p} \right] \quad [12]$$

$$\frac{\partial Stk_{Lc}}{\partial L_c} = \frac{-2 Stk_{Lc}}{L_c} \quad [13]$$

So the uncertainty of the Stokes number calculation is:

$$\delta Stk_{Lc} = Stk_{Lc} \left[\left(\frac{\delta Q}{Q} \right)^2 + \left(\left[\frac{2.52 \lambda + 2 D_p}{2.52 \lambda + D_p} \right] \left(\frac{\delta D_p}{D_p} \right) \right)^2 + \left(-2 \left(\frac{\delta L_c}{L_c} \right) \right)^2 \right]^{\frac{1}{2}} \quad [14]$$

where the uncertainties associated with L_c, D_p, Q are 0.5%, 5%, and 5% respectively.

$$\frac{\delta Stk_{Lc}}{Stk_{Lc}} = \left[(.05)^2 + \left(\left[\frac{2.52 \lambda + 2 D_p}{2.52 \lambda + D_p} \right] (0.05) \right)^2 + (-2 \cdot (0.005))^2 \right]^{\frac{1}{2}} \quad [15]$$

The performance of the CSVI units was evaluated over a range of particle sizes. Equation [14] above gives a peak error slightly larger than 11%. Figure 9 shows the variance of the uncertainty of the Stokes calculations.

Similarly the uncertainty of the collection efficiency calculation is determined below:

$$\eta_{collection} = \frac{Q_{exp} \cdot V_{exp} \cdot T_{exp} \cdot F_{exp}}{Q_{ref} \cdot V_{ref} \cdot T_{ref} \cdot F_{ref}} \quad [16]$$

Therefore, assuming negligible uncertainty in the time given by the stopwatch and using the uncertainty values found in Table 1:

$$\frac{\delta\eta_{collection}}{\eta_{collection}} = \left[\left(\frac{\delta Q_{exp}}{Q_{exp}} \right)^2 + \left(\frac{-\delta Q_{ref}}{Q_{ref}} \right)^2 + \left(\frac{\delta V_{exp}}{V_{exp}} \right)^2 + \left(\frac{-\delta V_{ref}}{V_{ref}} \right)^2 + \left(\frac{\delta F_{exp}}{F_{exp}} \right)^2 + \left(\frac{-\delta F_{ref}}{F_{ref}} \right)^2 \right]^{\frac{1}{2}} \quad [17]$$

$$\frac{\delta\eta_{collection}}{\eta_{collection}} = \left[(0.05)^2 + (-0.05)^2 + (0.001)^2 + (-0.001)^2 + \left(\frac{\delta F_{exp}}{F_{exp}} \right)^2 + \left(\frac{-\delta F_{exp}}{F_{exp}} \right)^2 \right]^{\frac{1}{2}} \quad [18]$$

The uncertainty of the fluorescence value varies with each experimental data point. While the fluorescence value obtained from the Turner Quantech Digital Filter Fluorometer (Model FM109515, Barnstead International, Dubuque, Iowa) for a single sample is consistent, several samples which should be identical may vary by as much as 10%. For example three reference samples taken consecutively under the same operating conditions may not produce the same fluorescence values due to random errors. The predicted uncertainty based on the Kline-McClintock analysis based on the range of fluorometer uncertainties shows the uncertainty for the efficiency calculation to lie between 7.2 and 15.28%.

RESULTS

Pressure Drop vs Flow Rate

The motivation for this study is to produce a high efficiency bioaerosol concentrator with relatively low power consumption. The power consumption is heavily dependant on the major flow pressure as can be seen from Equation [3]. The pressure drop was measured with an incline manometer as the volumetric flow rate was varied from 25-225 L/min. The pressure drop varied from 20 to 1000 pa. The pressure coefficient at the standard operating flow rate of 100 L/min was 1.4. The pressure drop vs flow rate curve for the first stage CSVI can be seen in Figure 10.

Efficiency Curves

The hindrance to efficiently collect particles larger than 8mm in previous virtual impactors was the existence of crossing trajectories of larger particles. As the particles are accelerated through the nozzle smaller particles are able to focus themselves within the jet. The larger particles are drawn towards the jet but have too much momentum to remain in the focused stream. Instead, the particles enter the stream through one side of the jet and continue on a linear path causing the particle to impact on the wall. An illustration of the potential path a large particle may take can be found in Figure 11. These losses associated with larger particles are the root cause seen for the drop in the efficiency curves found in previous studies (Haglund 2004).

Some geometric changes have been made to the virtual impactor nozzle based on numerical studies. The geometric changes allow the flow to be focused gradually. The gradual focusing leaves time for the more massive particles to enter and remain in the focused jet. The result is improved performance of the virtual impactor for particles as large as 13 μm AD.

First stage

The efficiency vs Stokes number for the first stage CSVI can be found in Figure 12. The first stage CSVI was found to be highly efficient for Stokes numbers ranging from 3.5 to 30.

Second stage

The second stage CSVI was found to behave very similarly to the first stage on a Stokes number basis. The efficiency vs Stokes number for the second stage CSVI can be found in Figure 13. The comparison of the first and second stages found in Figure 14 shows excellent agreement between the first and second stage CSVI units. The results show the ability to scale a CSVI unit to accommodate different flow rates without changing the overall concentration performance.

1st and 2nd stage CSVI in series

Figure 15 shows the performance of the first and second stage CSVI units when they operate in series. The results of the two stages acting in series show peak efficiencies above 90%.

Effect of Exposure to the Ambient Air of the CSVI Units

This experiment attempted to determine if prolonged exposure to ambient dust has an effect on the performance of a virtual impactor. This experiment was conducted by exposing a running second stage virtual impactor at 10 L/min to ambient dust for 48 hours and filtering all major and minor flows. In parallel a reference filter exposed to the same ambient dust was run at 10 L/min.

After forty-eight hours of continuous sampling of the ambient air in the laboratory the collection efficiency was measured for monodisperse 5 μ m AD particles. The results show that the CSVI was 85% efficient following the forty-eight hours of continuous

sampling. This efficiency is a 5-10% decrease in the collection efficiency compared to a clean unit.

The results of this experiment prove that the efficiency of a virtual impactor will decrease following prolonged exposure to ambient dust. It will therefore be necessary to implement a maintenance cleaning schedule for a continuous sampling system using a virtual impactor.

SUMMARY AND CONCLUSIONS

A two stage circumferential slot virtual impactor system was designed, manufactured, and tested. The effect of the improved geometry is evident in both the first and second stage units individually. The first and second stage had a 50% Stokes cutpoint of about 1.2 corresponding to a particle size of 2.5 μm . In series, the units provided peak efficiencies of 90%. This is a significant improvement over previous multiple stage virtual impactors operating at comparable flow rates and pressure drops. A second stage CSVI provides an efficient way of concentrating particles at lower flow rates. The behavior of a second stage CSVI is an excellent representation of the behavior of a larger CSVI intended to be operated at higher flow rates. The similarity in the results for a first and second stage CSVI also demonstrates the ability to scale a CSVI for different flow rates and multiple stages of concentration.

FUTURE RECOMMENDATIONS

Among the most significant discovery of this study is that a second stage CSVI with the accelerator resting on a diameter of about 8mm from its center is as efficient as the first stage which rests on about a 75mm diameter. The efficiency vs Stokes number curves show that the first and second stages indicate very similar behavior. It is also important to note that the success of a CSVI as a biological concentrator is contingent the success of a second stage CSVI. It my recommendation than new geometries and slot widths be tested with a second stage unit first. The smaller unit is indicative of the performance of a unit designed to handle a larger volume of air. The second stage can be manufactured quicker, cheaper and can be experimentally characterized easier. To minimize losses on the second stage CSVI ceiling, it may be necessary to draw the minor flow from both sides of the CSVI.

Geometric changes made should be incorporated into the Aerosol to Hydrosol Transfer Stage accelerator nozzle. The AHTS would also benefit from the improved ability to collect large particles.

REFERENCES

- Asgharian, B. and Godo, M. N. (1997). Transport and Deposition of Spherical Particles and Fibers in an Improved Virtual Impactor, *Aerosol Sci. and Technol.* 27:499-506.
- Chang, M-C., Geller, M. D., Sioutas, C., Fokkens, P. H. B., and Cassee, F. R. (2002). Development and Evaluation of a Compact, Highly Efficient Coarse Particle Concentrator for Toxicological Studies, *Aerosol Sci. Technol.* 36:492-501.
- Chein, H., and Lundgren, D. A. (1993). A Virtual Impactor with Clean Air Core for the Generation of Aerosols with Narrow Size Distributions, *Aerosol Sci. Technol.* 18:376-388.
- Chein, H., and Lundgren, D. A. (1995). A High-Output, Size-Selective Aerosol Generator, *Aerosol Sci. Technol.* 23:510-520.
- Chen, B. T., and Yeh, H. C. (1987). An Improved Virtual Impactor: Design and Performance, *J. Aerosol Sci.* 18:203-214.
- Ding, Y., Ferguson, S. T., Wolfson, J. M, and Koutrakis, P. (2000). Development of a High Volume Slit Nozzle Virtual Impactor to Concentrate Coarse Particles, *Aerosol Sci. Technol.* 34:274-283.
- Ding, Y., and Koutrakis, P. (2000). Development of a Dichotomous Slit Nozzle Virtual Impactor, *J. Aerosol Sci.* 31:1421-1431.
- Figuroa, E. O., McFarland, A.R., and Ortiz, C.A. (1982). Flattening Coefficients for DOP and Oleic Acid Droplets Deposited on Treated Glass Slides. *Amer Ind. Hyg. Assoc. J.* 43:395-399.
- Forney, L. J., Ravenhall, D. G., and Lee, S. S. (1982). Experimental and Theoretical

- Study of a Two-Dimensional Virtual Impactor, *Environ. Sci. Technol.* 16:492-497.
- Haglund, J. S., (2003). Two Linear Slot Virtual Impactors for Concentration of Bioaerosols. Ph.D. dissertation, Department of Mechanical Engineering, Texas A&M University, College Station, Texas.
- Haglund, J. S., Chandra, S., and McFarland, A. R. (2002). Evaluation of a High Volume Aerosol Concentrator, *Aerosol Sci. Technol.*, 36:690-696.
- Haglund, J. S. and McFarland, A.R. (2004). A Circumferential Slot Virtual Impactor, *Aerosol Sci Technol.*, 38:664-674.
- Han, R., and Moss, O. R. (1997). Flow Visualization Inside a Water Model Virtual Impactor, *J. Aerosol Sci.* 28:1005-1014.
- Hari, S. (2003). Computational Fluid Dynamics (CFD) Simulations of Dilute Fluid-Particle Flows. Ph.D. dissertation, Department of Nuclear Engineering, Texas A&M University, College Station, Texas.
- Hari, S. (2005). Simulations on the Second Generation Slot Virtual Impactors. (Unpublished Paper), Energy Systems Laboratory, Texas Engineering Experiment Station, Texas A&M University, College Station, Texas.
- Hounam, R. F., and Sherwood, R. J. (1965). The Cascade Centripeter: A Device for Determining the Concentration and Size Distribution of Aerosols, *Amer. Ind. Hyg. Assoc. J.* 26:122-131
- Lin, H., and Heintzenberg, J. (1995). A Theoretical Study of the Counterflow Virtual Impactor, *J. Aerosol Sci.* 26:903-914.
- Loo, B. W., and Cork, C. P. (1988). Development of High Efficiency Virtual Impactors,

- Aerosol Sci. Technol.* 9:167-176.
- Marple, V.A. (2004). History of Impactors-The First 110 Years. *Aerosol Sci. Technol.* 38:247-292.
- Marple, V. A., and Chien, C. M. (1980). Virtual Impactors: A Theoretical Study, *Environ. Sci. Technol.* 14:976-985.
- Masuda, H., Hochrainer, D., and Stober, W. (1979). An Improved Virtual Impactor for Particle Classification and Generation of Test Aerosols with Narrow Size Distributions, *J. Aerosol Sci.* 10:275-287.
- Moncla, B. (2004). A Study of Bioaerosol Sampling Cyclones. M.S. Thesis, Department of Mechanical Engineering, Texas A&M University, College Station, Texas.
- Phan, H. N., McFarland, A. R. (2004). Aerosol-to-Hydrosol Transfer Stages for Use in Bioaerosol Sampling, *Aerosol Sci. Technol.* 38:300-310.
- Romay, F.J., Roberts, D.L., Marple, V.A., Liu, B.Y.H., and Olsen, B.A. (2002). A High-Performance Aerosol Concentrator for Biological Agent Detection. *Aerosol Sci. Technol.* 36:217-226.
- Ravenhall, D. G., Forney, L. J., and Hubbard, A. L. (1982). Theory and Observation of a Two-Dimensional Virtual Impactor, *J. Colloid Interface Sci.* 85:508-520.
- Ravenhall, D. G., Forney, L. J., and Jazayeri, M. (1978). Aerosol Sizing with a Slotted Virtual Impactor, *J. Colloid Interface Sci.* 1:108-117.
- Sioutas, C., Koutrakis, P., and Burton, R. M. (1994a). Development of a Low Cutpoint Slit Virtual Impactor for Sampling Ambient Fine Particles, *J. Aerosol Sci.* 25:1321-1330.
- Sioutas, C., Koutrakis, P., and Burton, R. M. (1994b). A High-Volume Small Cutpoint

Virtual Impactor for Separation of Atmospheric Particulate from Gaseous
Pollutants, *Particle Sci. and Technol.* 12:207-221.

APPENDIX



Figure 2: Photograph of CSVI stage 1 and 2.



Figure 3: Inside of first and second stage CSVI units.

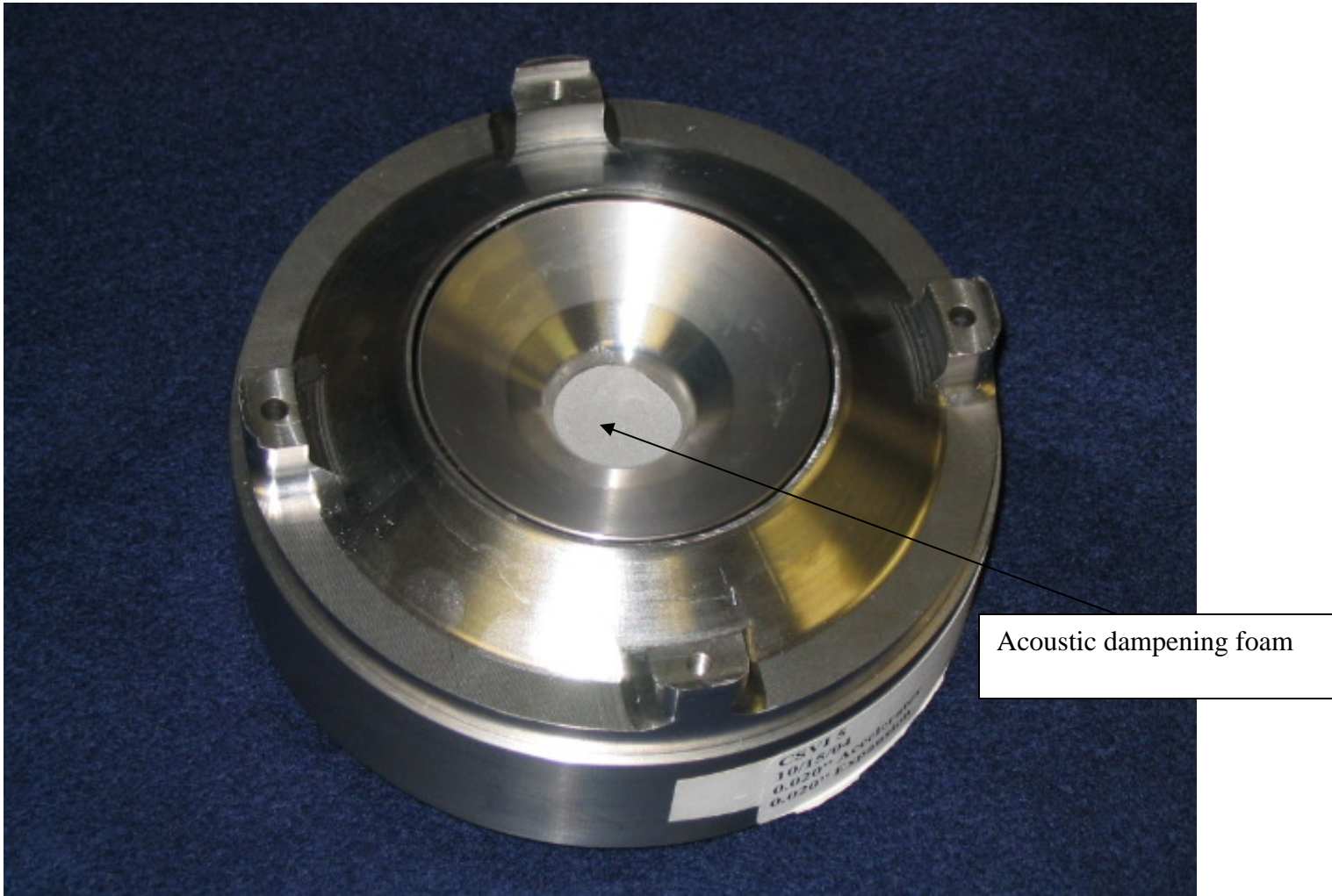


Figure 4: Acoustic absorbing open face foam in the center of the first stage CSVI.

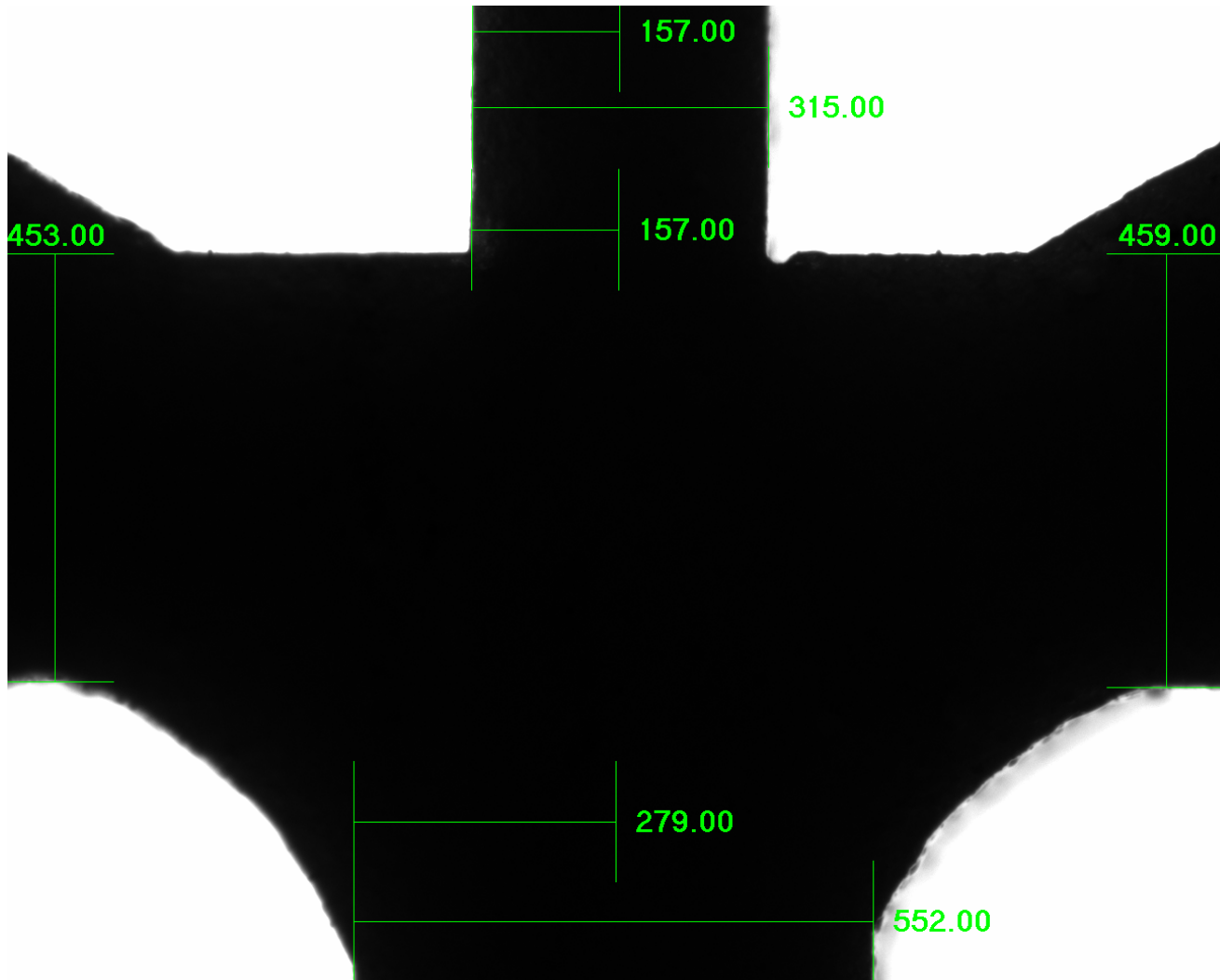


Figure 5: Rubber casting of the first stage critical region.

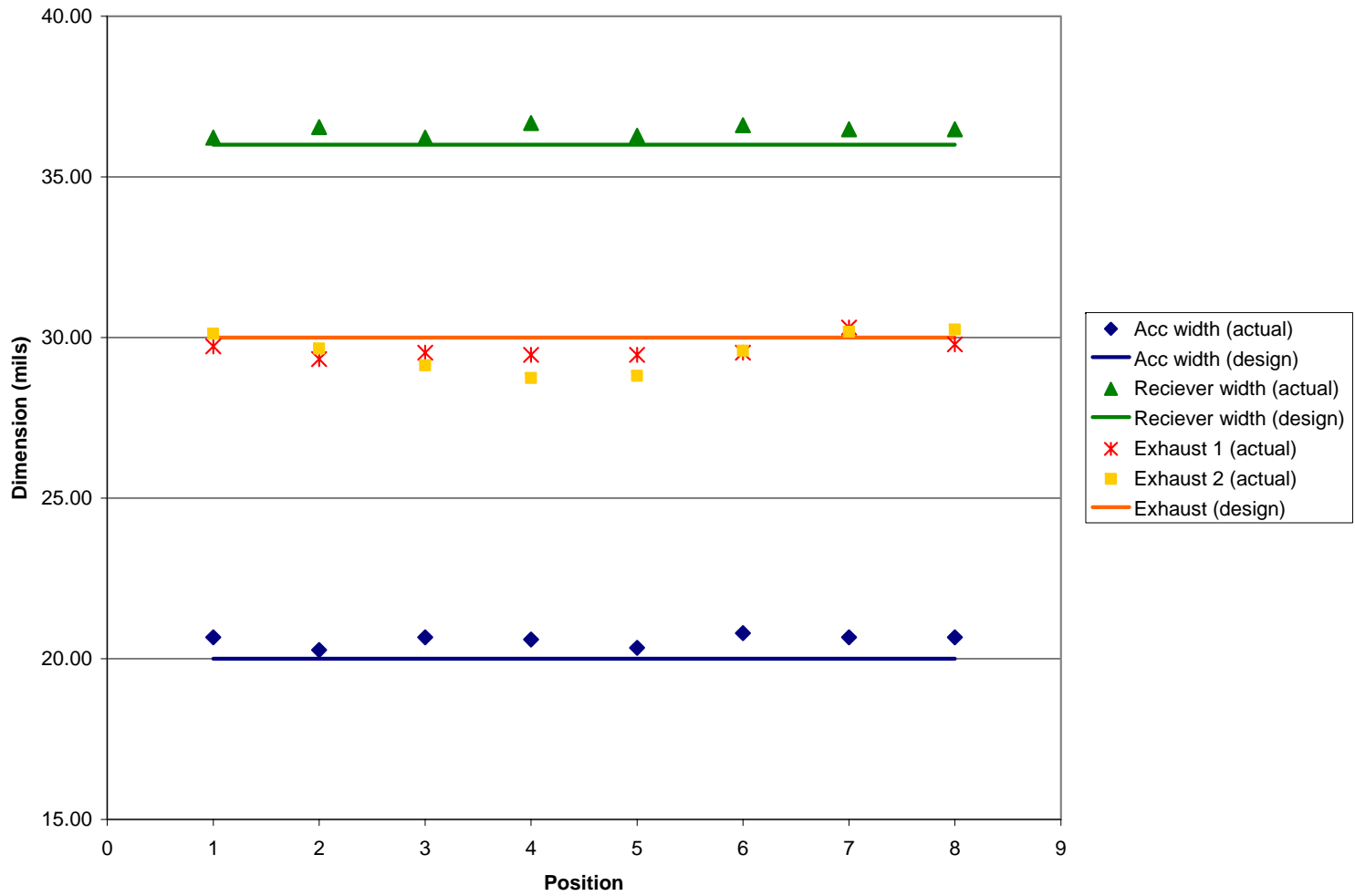


Figure 6: Measured values compared to designed values for stage 1 CSVI. Courtesy C. Adams (Aerosol Technology Laboratory, College Station, TX)

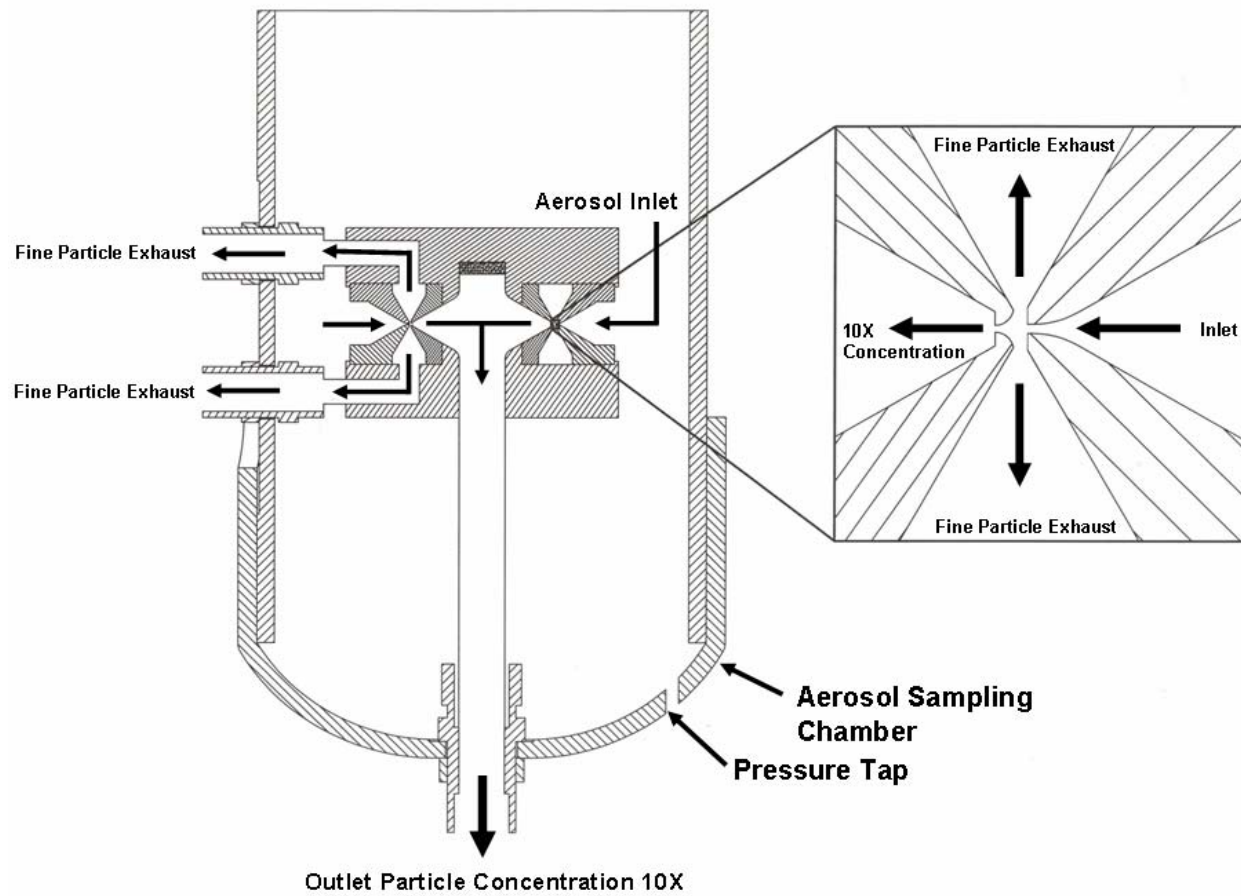


Figure 7: CSVI aerosol sampling chamber.

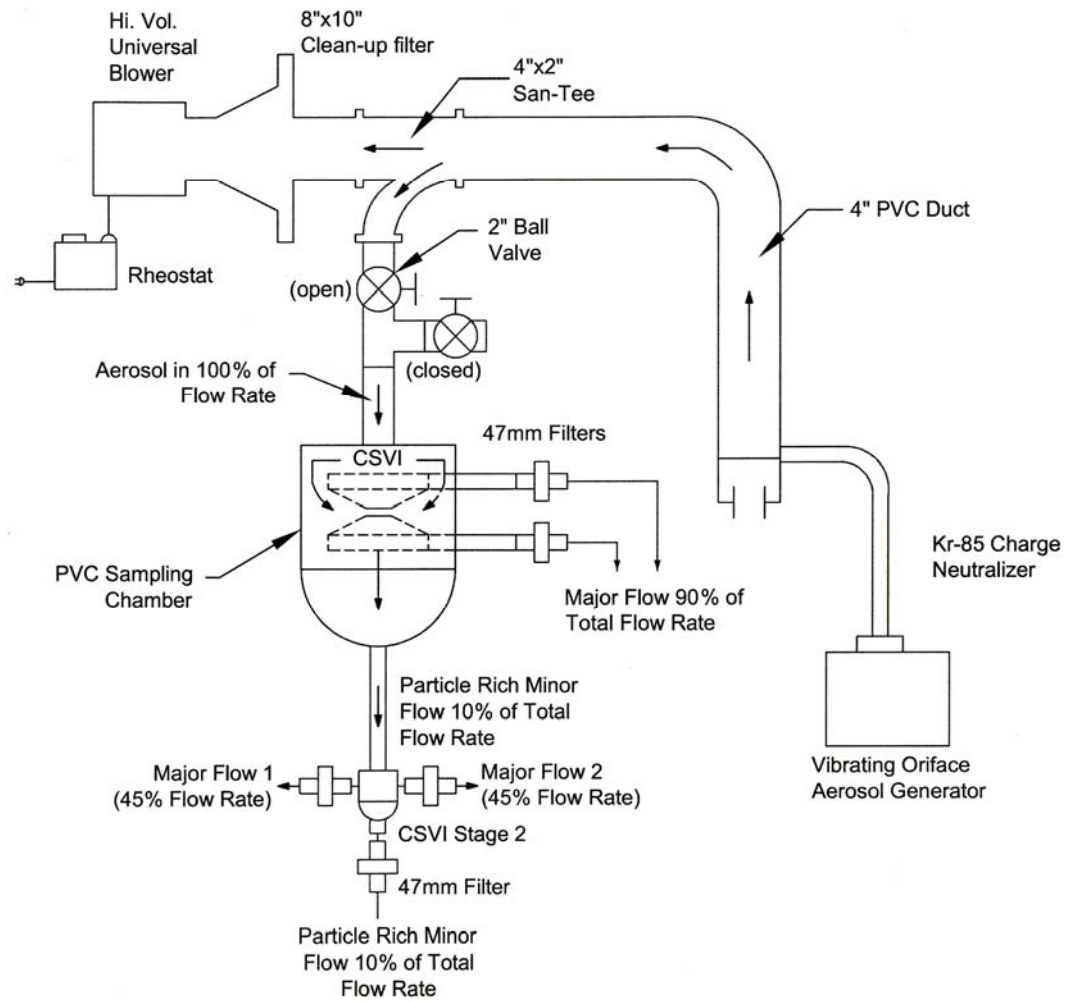


Figure 8: Complete flow system for CSVI stage 1 and 2.

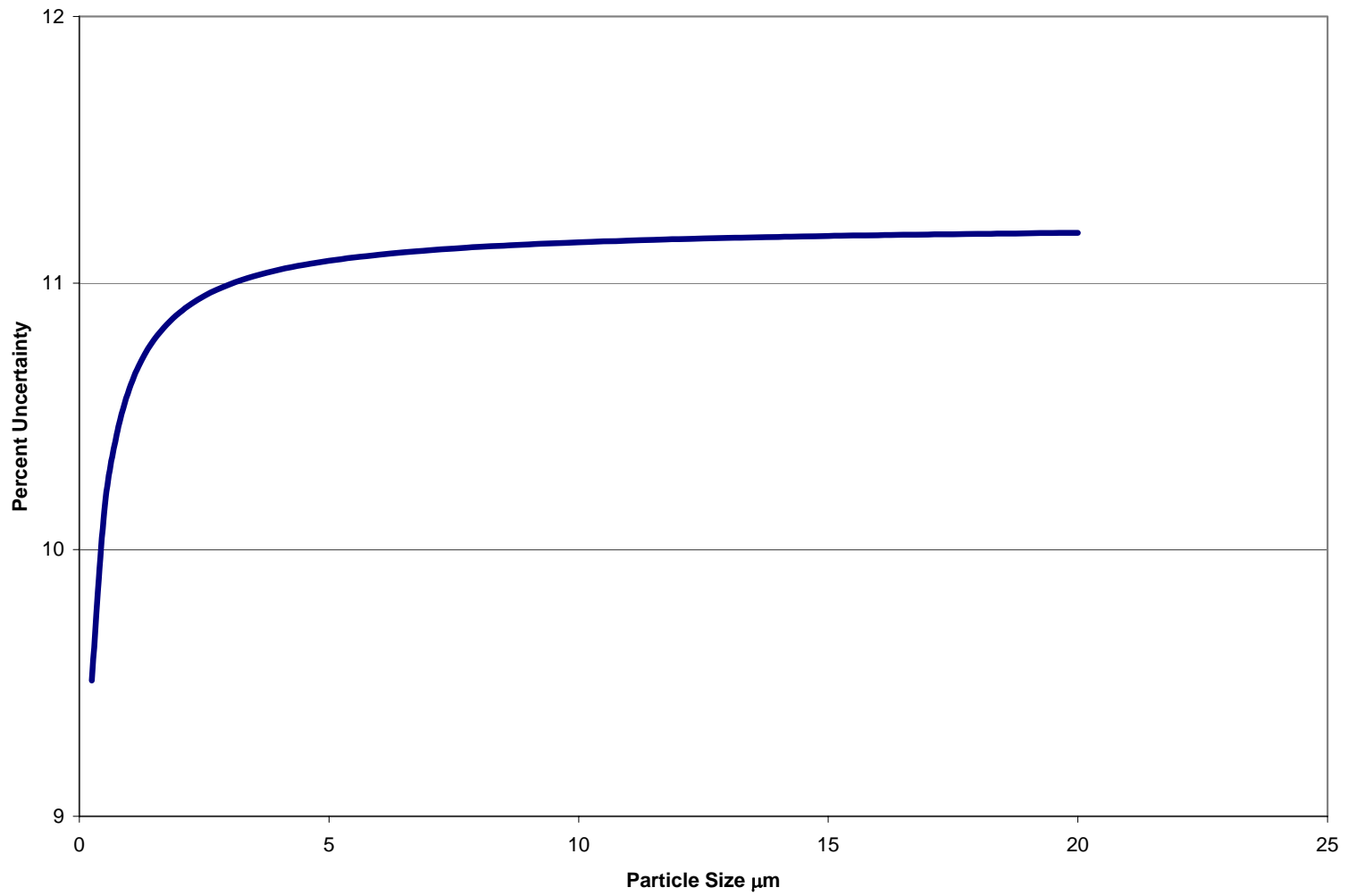


Figure 9: Predicted uncertainty in Stokes calculation by Kline-McClintock.

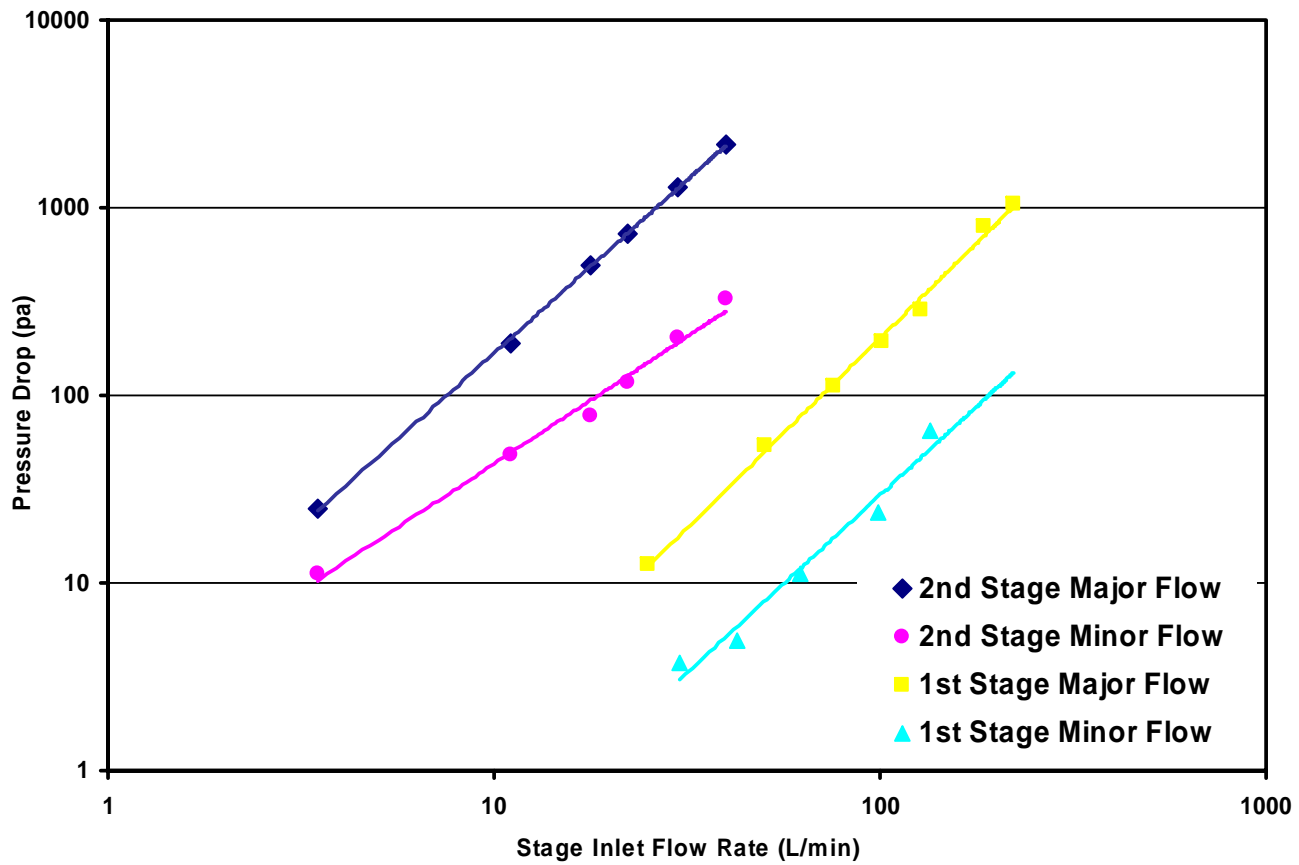


Figure 10: Pressure drop vs flow rate for first stage CSVI.

Entrance Flow Containing Large and Small Particles

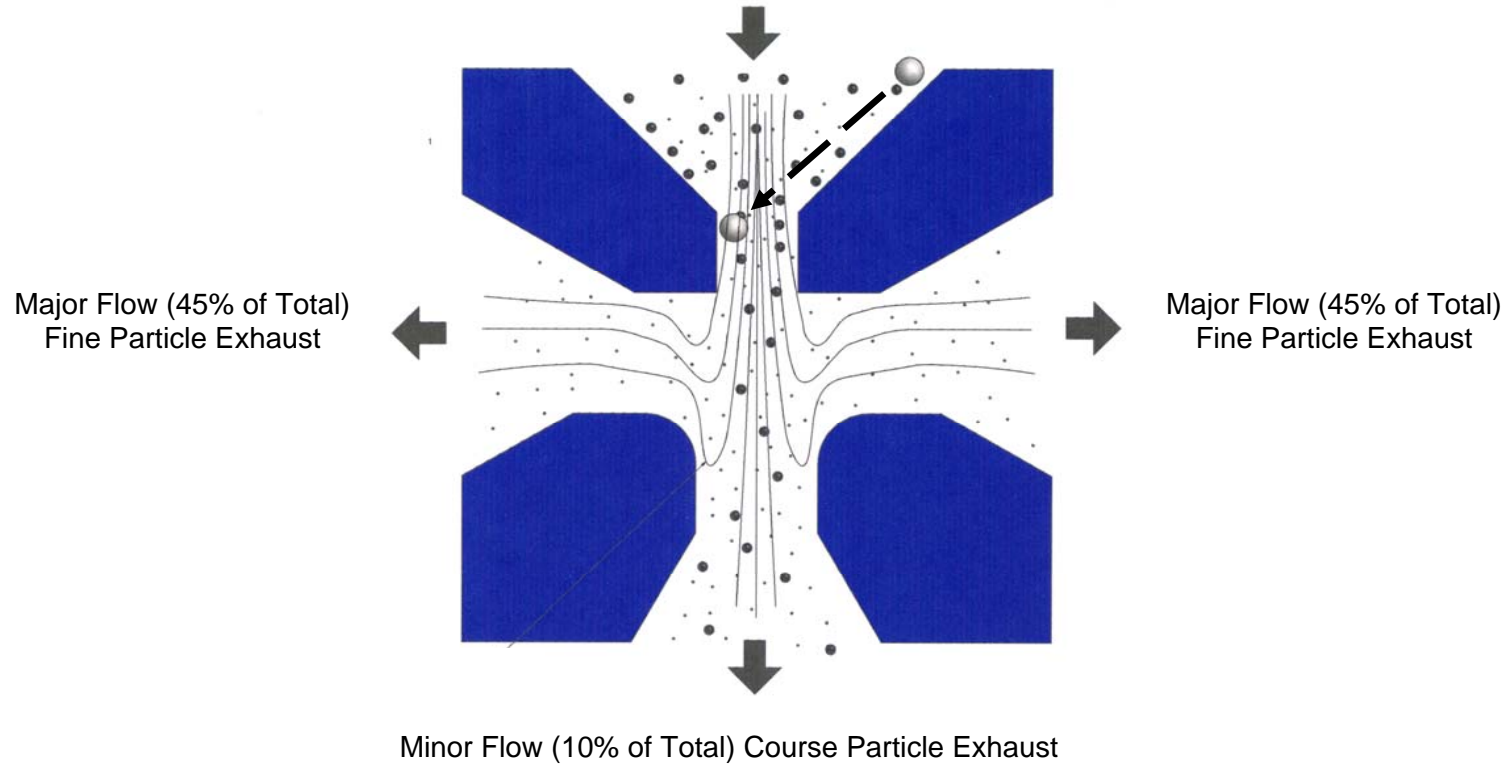


Figure 11: Illustration of crossing trajectories of larger particles.

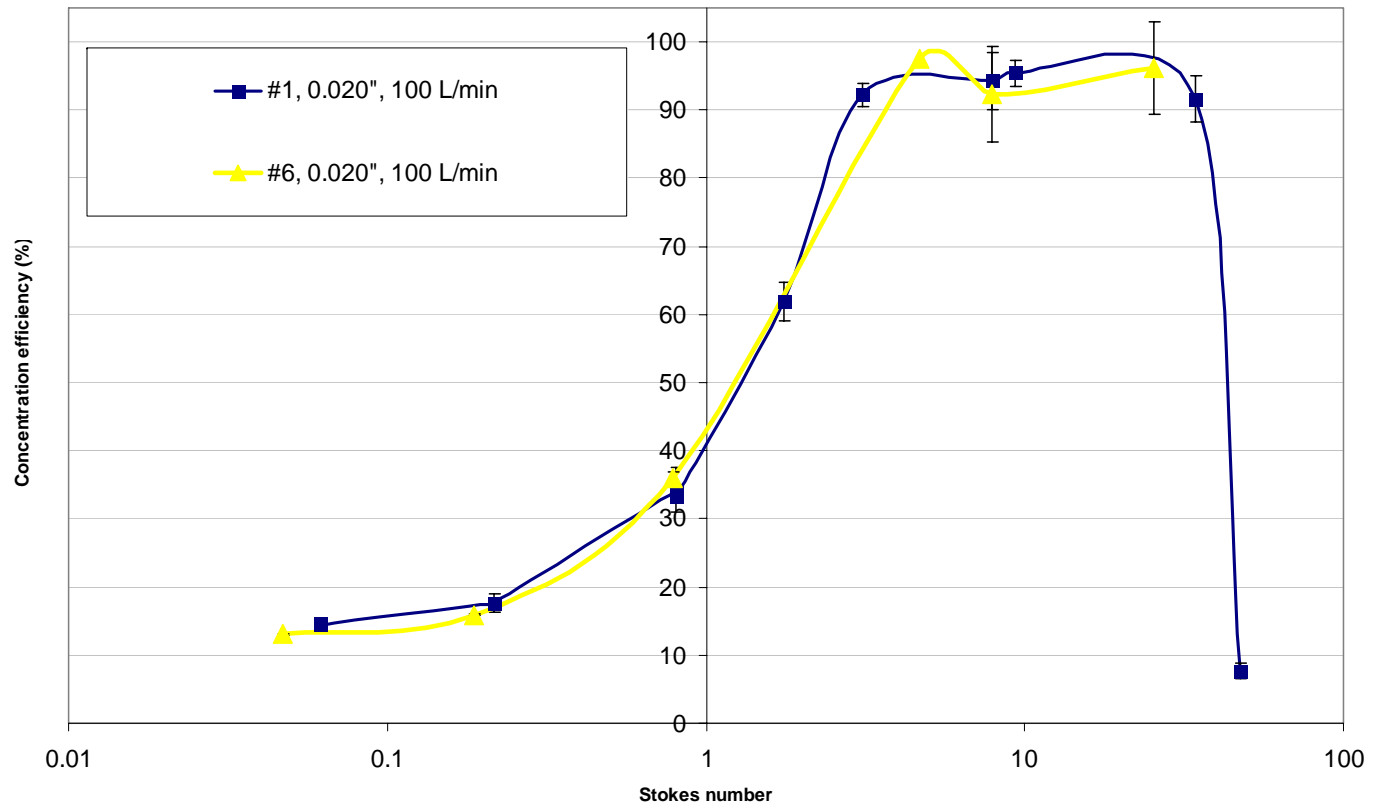


Figure 12: Performance of the first stage CSVI.

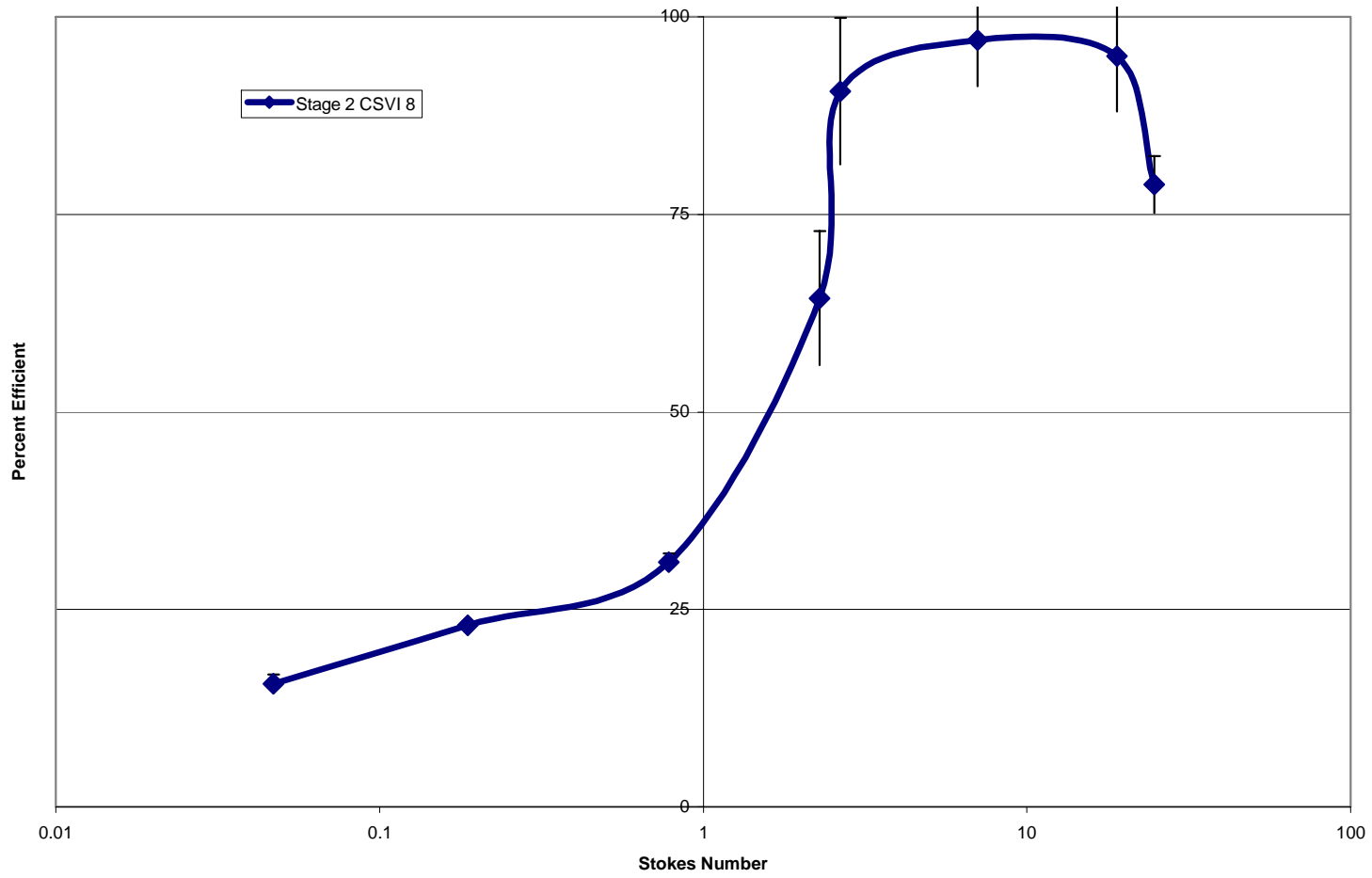


Figure 13: Performance of second stage CSVI.

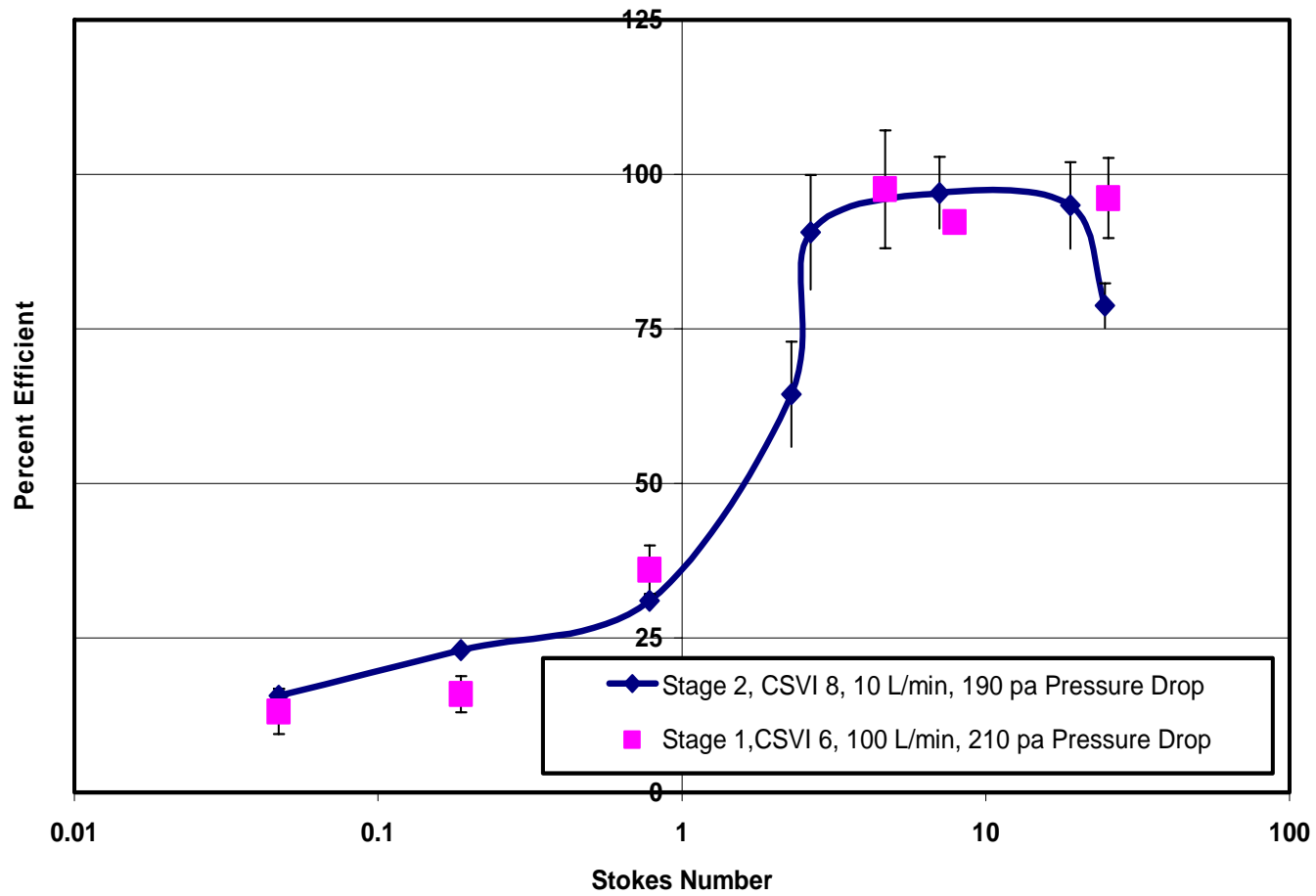


Figure 14: Comparison of first and second stage CSVI units.

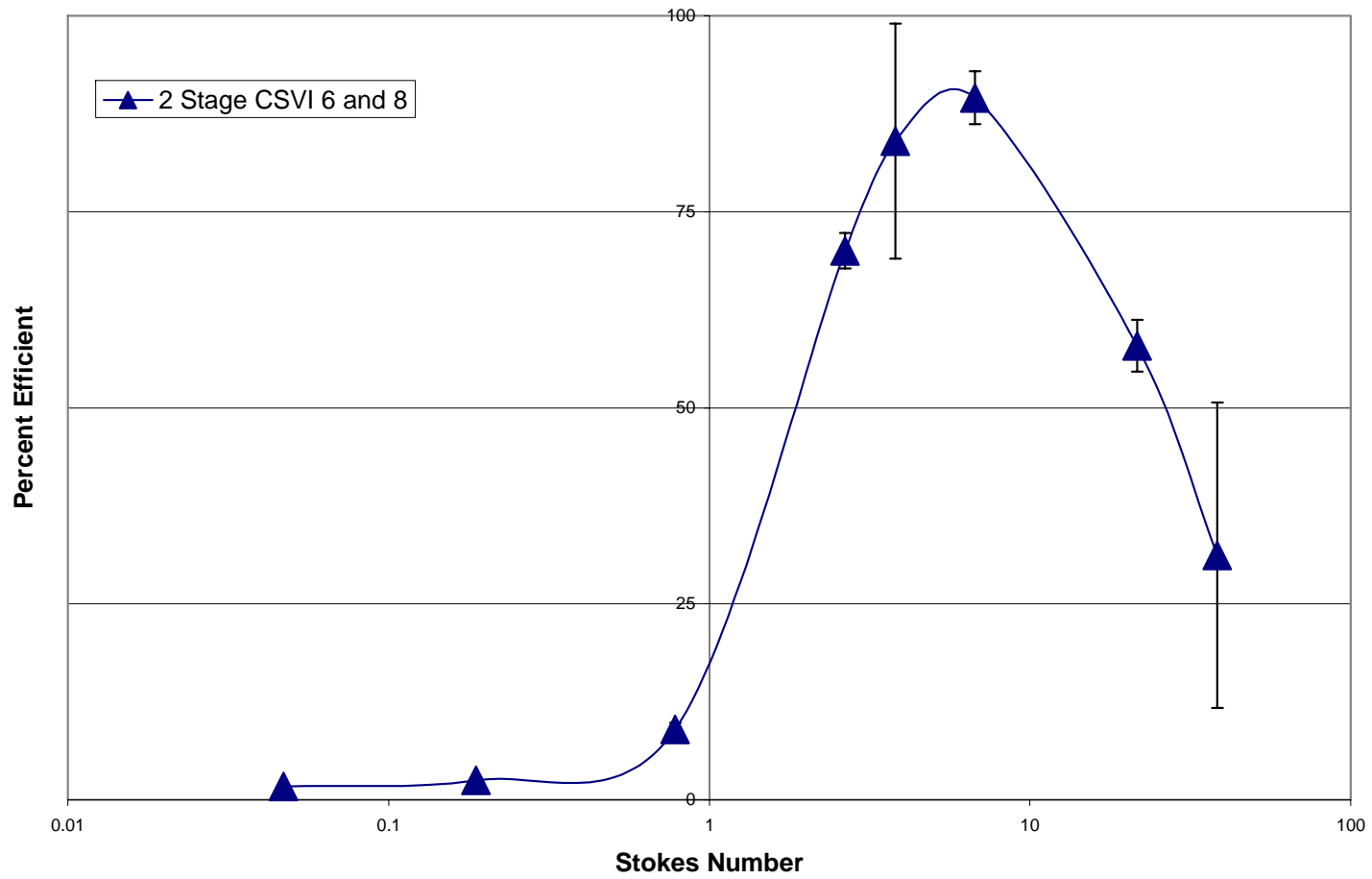


Figure 15: First and second stage CSVI plots.



Figure 16: Demonstration of ability of second stage to be nested within the first stage.

Table 1: Uncertainties used for Kline McClintock Uncertainty Analysis

RMC Rate-Master Flowmeter Accuracy	2% (Dwyer Catalog 99)
RMC Rate-Master User ability to determine flow	2% (Dwyer Catalog 99)
Fluorometer Value	1-10% (from coefficient of variations of data)
REPIPET® DISPENSER, Barnstead	0.1% (barnsteadthermolyne.com)
Particle Sizing PSL	4% (Duke Scientific)
Particle Sizing Oleic Acid	5%

Table 2: Measurements from first stage CSVI

First Stage CVSI [μm]					
Pos	Accl.	Rec.	L Exh	R Exh	A-R Offc.
1	508	905	745	760	8
2	518	927	747	760	10
3	522	917	755	740	10
4	523	932	757	748	16
5	520	918	750	730	6
6	530	933	747	752	8
7	523	917	748	775	10
8	527	935	752	777	16

Courtesy C. Adams (Aerosol Technology Laboratory, College Station, TX)

VITA

Name: Refugio Rey Isaguirre IV

Date and Place of Birth: June 5, 1981
McAllen, TX

Educational Background: Bachelor of Science in Mechanical Engineering
(May 2003)
Texas A&M University
College Station, TX

Address: P.O. Box 6191
McAllen, TX 78502